J. Inst. Eng. India Ser. A (December 2022) 103(4):1147–1164
https://doi.org/10.1007/s40030-022-00685-7

ORIGINAL CONTRIBUTION

Laboratory Investigations to Optimize the Physicochemical Parameters for *Bacillus cereus* Inclusions in Concrete for Enhanced Compressive Strength and Chloride Resistance

Sk Rahaman[1] · Jayati Ray Dutta[1] · Mohna Bandyopadhyay[2] · Arkamitra Kar[1]

Received: 19 April 2022 / Accepted: 25 August 2022 / Published online: 6 October 2022

Abstract A popular technique for improving the properties of concrete in recent times is microbial inclusion. Calcite precipitated by the metabolic activities of these microbes reduces the porosity of concrete and enhances its compressive strength and chloride resistance. In this study, the suitability of *Bacillus cereus* as a potential microbe in concrete environment is determined using laboratory experiments. Due to the absence of reported information, this study optimizes the inoculum volume, substrate volume, and pH required for growth of *Bacillus cereus*, prior to inclusion in concrete. The optimal proportions of bacterial solution to improve the compressive strength and chloride resistance are determined. Additionally, the optimal quantity of calcium lactate nutrient required for bacterial growth in concrete are also determined. It is observed that addition of 1% solution of *Bacillus cereus* in concrete results in 14–23% increase in compressive over a period of 90 days. Additionally, it is observed that the corresponding reduction in chloride permeability is nearly 19% compared to traditional concrete. These findings are validated using mineralogical, chemical, and microstructural analyses.

Keywords Bacterial concrete · *Bacillus cereus* · Growth optimization · Splitting tensile strength · Chloride permeability · Water sorptivity

✉ Sk Rahaman
p20180416@hyderabad.bits-pilani.ac.in

[1] Birla Institute of Technology and Science (BITS)-Pilani, Hyderabad Campus, Hyderabad, Telangana 500078, India

[2] Department of Dermatology, University of Pittsburgh, Pittsburgh, PA 15260, USA

Introduction

The popularity of concrete in recent years due to rapid infrastructure development has resulted in an annual portland cement (PC) production of 3.27 billion tons [1]. Simultaneously, the annual investment towards maintenance and repair of concrete structures amounts to nearly 0.52% of the US Annual GDP, with the respective figures for India and China being 1.08% and 5.57% as of 2018 [2]. The production of PC and aggregates used in concrete consumes enormous amounts of energy and emits equivalent CO_2, reportedly 1.50 ± 0.12 GT that is almost 4% of the global fossil fuel emissions [3]. Due to anticipated doubling of these numbers by the end of this decade [4], it is of utmost importance to enhance the mechanical and long-term characteristics of concrete structures [5]. Although PC is a widely used construction material, various factors such as excessive load, mechanical stress, shrinkage, and chemical attack make it susceptible to microcracks that expand over time and reduce its service life [6]. One of the possible techniques to reduce the need for PC concrete maintenance and reduce environmental disruption is microbial inclusion in the form of calcite precipitating bacteria [7]. However, there are limited reports on the practical applications of this technique. Additionally, there are no systematic reports on optimizing the physicochemical parameters influencing the growth of bacterial strains in a concrete environment. Hence, the focus of this study is determination of the optimal parameters for development of microbial inclusions in PC concrete to improve its properties. The bacterial strain selected for this study is *Bacillus cereus* and its optimal concentration for addition in concrete is determined using physicochemical parameters, namely substrate volume, inoculum volume and pH. Further experimental findings from mechanical and

chemical analyses of concrete with bacterial inclusions are corroborated with microstructural characteristics.

Existing research reports that enhancement of concrete properties has been attempted using several techniques involving synthetic polymers such as epoxy treatment or latex modified concrete [8]. But they are highly non-biodegradable and harmful to the environment, warranting the use of an alternative biological repair technique in concrete [8–13]. The current trend is using calcite- or calcium carbonate-precipitating bacteria to occupy the pores and impart a self-healing capacity to the concrete [8–14]. When the pores are occupied by the bacterial colonies growing inside them, the pore volume is reduced which refines the microstructure, thereby increasing the resistance to chloride ion penetration. This technique is called microbially induced calcite precipitation (MICP) and it is usually achieved through ureolytic bacteria [15]. It is essential to mention here that the pH inside a traditional PC concrete environment is around 13.3 and the internal temperature of concrete varies from 37 to 40 °C [16]. As a result, the selected microorganism must be able to resist the high alkalinity and the internal temperature of the concrete environment [17].

Reportedly, gram-positive spore-forming bacteria can survive high pH and various stress-related to concrete [13]. Research has shown that the most commonly used bacteria to satisfy this requirement are *Bacillus subtilis* JC3 obtained from soil [8–14]. The main reasons for choosing these bacteria are their ability to form spores which are viable for germination even after the initial colonies are used up and also their ability to precipitate calcium carbonate crystals through urease enzyme activity. *Sporosarcina pasteurii* has also been used by some researchers for this purpose [12]. It is reported that the bacterial concentration is directly proportional to the durability performance of PC concrete [18]. However, more recent studies have reported that a concentration of 10^5 cells per ml results in the maximum compressive strength gain for mortar specimens [9]. It is also observed that *Bacillus sphaericus* helps in converting urea into carbonate and ammonium, resulting in MICP [19]. MICP facilitates the repair of microcracks and by filling the pores [17]. These findings were confirmed by other studies [20]. It is also found that the addition of calcium lactate as a nutrient for the bacteria promotes urease activity and results in further calcium carbonate precipitation which assists crack healing [21]. Once the cracks are healed with calcium carbonate, the bacterial cells become dormant in the absence of aerobic conditions. If new cracks start to appear, these cells become functional once again and heal them through MICP [22]. Additionally, this calcite deposition in the voids improves the strength and reduces concrete gas and water permeability [23]. A study using *Bacillus sphaericus* stated that the reduction of water permeability due to calcite deposition is in the range of 65% to 90% [15]. However, studies also report bacterial inclusions in concrete reduce water absorption by 48% to 55% and porosity by 50% to 55% [24]. Furthermore, MICP can prevent reinforcement corrosion in the absence of Cl^- ions due to crack healing, increasing the service life of reinforcement inside the concrete [25]. These changes in mechanical and chemical properties of PC concrete are attributed to the corresponding modifications in microstructure due to bacterial inclusions. The metabolic activity of the bacterial strains in presence of a conducive aerobic environment and nutrients precipitates calcite, as represented by Eq. (1) [7].

$$Ca(C_3H_5O_2)_2 + 7O_2 \rightarrow CaCO_3 + 5CO_2 + 5H_2O \quad (1)$$

Mineralogical, chemical, and microstructural analyses show that the mineralogical composition and the microstructure of hardened PC paste undergo significant modifications due to this MICP [13, 24–26]. Existing research shows the formation of calcite layers using X-ray diffraction (XRD) analysis of cracked concrete incorporated with *Bacillus sphaericus* cured in a solution of 2% urea and 25 mM $CaCl_2$ per ml of water [26]. The resulting white precipitation due to metabolic activity of the bacteria in the cracked surface exhibited diffraction patterns corresponding to calcite [27]. A study using scanning electron microscopy (SEM) demonstrated the presence of calcite crystal in hardened cementitious paste specimens impregnated with *S. pasteurii* [14]. Another study reported the presence of calcite crystal in rod-shaped structure in specimens prepared with *Bacillus sphaericus* using scanning electron micrographs [28]. Hence, a combination of XRD and SEM and also Fourier transform infrared (FTIR) are used in the present study to correlate the microstructural characteristics of hardened paste samples with the mechanical properties of concrete specimens including bacterial inclusions.

It is extensively reported that bacterial growth and metabolic activity resulting in MICP require specific conditions of temperature, relative humidity, pH, and nutrient volume. Hence, this technique is currently rendered suitable for precast members constructed under controlled conditions [29]. To overcome the limited use of bacteria in concrete under laboratory conditions and encourage widespread practical usage of this technique, the present study adopts a direct method of bacterial incorporation in concrete. *Bacillus subtilis* is reportedly the most commonly used bacterial strain for incorporation in PC concrete. However, a previous study by the present authors showed that the growth of *Bacillus cereus* takes place at a greater rate than *Bacillus subtilis* at high pH [29]. The same study also identified the prescribed growth parameters and established the potential for *Bacillus cereus* for inducing MICP in PC concrete. Hence, *Bacillus cereus* is selected as the bacterial strain for inclusion in concrete as part of the present study.

To the best of the knowledge of the authors of this proposal, there is no reported ASTM or Indian standard on optimizing the parameters for the growth and development of bacterial inclusions in concrete. Simultaneously, there are no standard codes of practice for the mix design and mixing proportions for this type of concrete. Moreover, there are limited studies on the long-term properties of bacterial concrete.

Hence, this study aims to establish the optimal physicochemical parameters for bacterial growth in concrete, to encourage further practical application of this technique in real life. To achieve this goal, it is of utmost importance to minimize the effort required for preparation of the bacterial cultures and the cost of repeated trials for obtaining the suitable bacterial concentration in concrete. Hence, the specific objectives of this study are: (i) to determine the optimal values of substrate volume, inoculum volume, and pH required for the growth of *Bacillus cereus* in PC concrete environment; (ii) to determine the optimal amount of calcium lactate as an additional nutrient to aid in the growth of *Bacillus cereus*, based on observations from compressive strength, splitting tensile strength, rapid chloride permeability tests (RCPT), and water sorptivity; (iii) to determine the optimal concentration of *Bacillus cereus* in PC concrete for enhancing the aforementioned characteristics of PC concrete; and (iv) to correlate the changes in compressive strength and RCPT of bacterial concrete specimens with the corresponding microstructural changes in hardened paste samples of PC due to same bacterial inclusions. The outcome of this study is a suitable mix design for PC concrete admixed with optimal concentrations of *Bacillus cereus* and calcium lactate for enhanced compressive strength, splitting tensile strength, reduced chloride permeability and water sorptivity.

Material and Methodology

In this study, two different sets of materials and methodology were used simultaneously to conduct experiments related to the bacterial growth parameter optimization and the durability performance of bacterial concrete.

Material

Material for Bacterial Optimization

For this study, lyophilized glass vials containing *Bacillus cereus* MTCC 430 were procured from the Microbial Type Culture Collection and Gene Bank (MTCC) India. Miller Luria Bertani (LB) broth containing 10 g of tryptone, 5 g of yeast extract, and 10 g of NaCl per 1 L of distilled water produced in the laboratory was used for culture media preparation. NaOH and diluted HCl solution was used to adjust the pH of LB broth. Locally procured calcium lactate was used as a nutrition source for bacteria inside the concrete.

Table 1 Chemical composition of cement

Ingredients	Percentage
Lime (CaO)	66.26
Silica (SiO_2)	18.75
Alumina (Al_2O_3)	4.27
Ferric oxide (Fe_2O_3)	4.16
Sulphuric anhydride (SO_3)	3.22
Magnesium oxide (MgO)	1.41
Sodium oxide (Na_2O)	0.77
Potassium oxide (K_2O)	1.16

The fineness of the PC used is 225 m^2/kg

Table 2 Properties of the aggregates

Table aggregate	Water absorption (%)	Specific gravity	Fineness modulus	Aggregate impact value (%)	Aggregate abrasion value (%)
FA	0.5	2.65	3.028	–	–
CA	0.1	2.72	6.863	31.71	25.6

Materials for Concrete

PC grade 53 conforming to IS 269-2015 [30] (equivalent to type I of ASTM C150-21 [31]) was used for this study. The chemical composition derived from the X-ray fluorescence spectroscopy (XRF) analysis given in Table 1. Fine aggregate (FA) conforming to Zone II as per IS 383-2016 [32] and equivalent to ASTM C33/C33M-18 [33] was obtained from the nearest river bed. Locally available crushed granite (nominal size 20 mm) conforming to ASTM C33/C33M-18 [33] was used as coarse aggregate (CA) in this study. In Table 2, the physical properties of both CA and FA are presented.

Methodology

Revival of Bacterial Strain and Gram Staining

The lyophilized bacterial strain collected from MTCC India was first revived for preparing an active culture. A 50 mL falcon tube containing 5 mL of LB broth was prepared and sterilized in an autoclave setup. After the sterilization, glass vials containing the lyophilized strain were broken gently. A small amount of culture was inoculated in 10 mL LB broth in a 50 mL falcon tube under laminar airflow using laminar airflow a sterile needle-type inoculum loop. Soon after inoculation, the falcon tube was stored inside an orbital shaking

incubator at 37 °C with an RPM of 120 for 24 h. These settings were obtained from existing literature [34]. After 24 h of growth, the culture media was checked using gram staining [35] to detect any contamination in the culture. A small amount of culture was taken on a glass slide for gram staining, spread evenly to prepare a smear of bacteria, and heat-fixed using a Bunsen burner. After heat-fixing, the glass slide was flooded with gram's crystal violet reagent for one minute and washed with water. It was then saturated with gram's iodine for another 1 min and washed with decolourizer, following washing with water. Finally, it was counterstained with safranin and the glass slide was air-dried. Then, it was observed under a compound microscope for checking any contamination [36]. Microscopic images of *Bacillus cereus* captured using a compound microscope are shown in Fig. 1a. The observation of a purple-blue color confirmed gram-positive strain and is consistent with findings from previous research [34].

Once the culture was revived and the absence of contamination was confirmed, the stock culture was prepared in agar plate as shown in Fig. 1b. A loopful of culture inoculated in a conical flask containing 50 mL of LB and kept in incubator. When an optical density of 0.4 was achieved during the growth phase of the bacterial strains, 500 µL of the culture along with 500 µL of 50% glycerol stock was blended in a 1 mL Eppendorf tube at a temperature of − 80 °C for further use. The primary culture was then inoculated for preparation of the bacterial solution for inclusion in concrete.

Methods for Bacterial Growth Optimization

As mentioned earlier, three different physicochemical parameters, namely inoculum volume (IV), substrate volume (SV), and pH, were selected for optimization in this study. For each optimization, triplicate specimens were tested. For the IV optimization, four different concentrations of the primary culture, i.e., 0.5%, 1%, 1.5%, and 2% w.r.t LB broth (vol/vol), were selected to begin the tests. These mixes are denoted as IV 0.5, IV 1.0, IV1.5, and IV2.0, respectively. 100 mL of LB broth was prepared in a screw cap conical flask and kept inside an autoclave chamber at a temperature of 120 °C for 90 min. Then, the autoclaved LB broth was inoculated separately inside a pre-fabricated laminar airflow chamber to avoid contamination with the said percentages containing 10^7 to 10^{11} colony forming units per ml (cfu/mL). Immediately after the inoculation, the conical flask was transferred into an orbital shaking incubator at a maintained temperature of 37 °C and a shaking speed of 120 rpm for a period of 24 h. From the inoculation, the optical density (OD) of the culture media was measured at an interval of every two hours. The corresponding bacterial growth curves are presented in Fig. 3.

For the SV optimization, four different quantities of LB, i.e., 10 g, 15 g, 20 g, and 25 g, were taken for each 1000 mL of distilled water. These mixes are denoted as SV10, SV15, SV20, and SV25, respectively. The bacterial growth curves were recorded and the quantity of SV was optimized. The corresponding bacterial growth curves are presented in Fig. 4.

For the pH value optimization, the bacterial growth curves were recorded at four different pH values of 6.0, 7.0, 8.0, and 9.0. These mixes are denoted as pH 6, pH 7, pH 8, and pH 9, respectively. The corresponding bacterial growth curves are presented in Fig. 5.

Concrete Mix Proportions and Specimen Preparation

Mix Proportions

A control PC concrete mix conforming to grade M40 was prepared using the recommendations of ACI 211.1-91 [37] for this study. The resultant mix proportions were verified using the recommendations of IS 10262: 2019 [38]. The control concrete mix proportions were modified by replacing

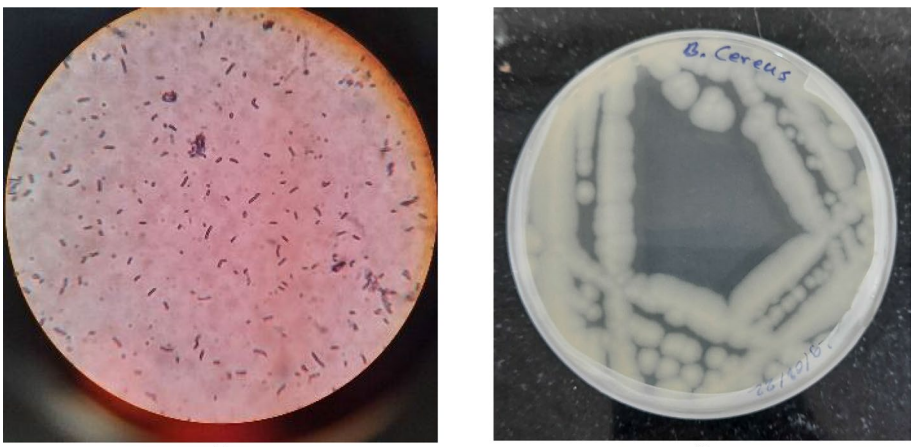

(a) (b)

Fig. 1 **a** Microscopic image of *Bacillus cereus* (gram-positive, rod-shaped), **b** Stock culture plate of *Bacillus cereus*

only the water content with the requisite concentrations of bacterial cells to prepare the bacterial concrete mixes. The necessary quantity of CL was added to the concrete mix as per requirement. The detailed calculations are provided as supplementary information. Ten concrete mixes with varying percentages of calcium lactate (CL) and *Bacillus cereus* (BC) culture media were prepared and characterized for this study. CL proportions were varied as 0.5%, 1% 1.5%, and 2% w.r.t. weight of PC. These mixes are denoted as 0.5% CL, 1% CL, 1.5% CL, and 2% CL, respectively. BC culture media were varied as 0.5%, 1% 1.5%, and 2% w.r.t. the total water content in the PC concrete mix. These mixes are denoted as 0.5% BC, 1% BC, 1.5% BC, and 2% BC, respectively. Finally, another mix was prepared with the optimal proportions of CL and BC to identify the influence of lactate on bacterial growth in concrete. This mix is denoted as BC + CL. The detailed mix proportions are presented in Table 3.

Mixing Procedure

The dry materials comprising the coarse and fine aggregates were blended using a planetary mixer to achieve a uniform blend. Once homogeneity was achieved, two-thirds of the total water content containing the bacterial cells were added to the dry mix and the planetary mixer was run for three minutes. Subsequently, the dry PC and calcium lactate were added and mixed uniformly. This was followed by adding the remaining water and another two minutes of mixing to obtain a uniform workable mix. Slump tests were conducted for each mix. The results for the optimal mix are presented in Fig. 8b along with the corresponding compressive strength results. Triplicate specimens were then cast for compressive strength testing and RCPT. They were demoulded after 24 h and stored in a curing tank for 28 days at an ambient average lab temperature of 31 ± 2 °C and relative humidity ranged from 55 to 65%. The bacteria incorporated samples are cured separately to avoid contamination. The specimens were tested at 7, 28, and 90 days, respectively, to determine each of the aforementioned characteristics and the result obtained presented in Fig. 5.

Preparation of Specimens for Microanalyses

The paste samples were prepared under controlled conditions for microstructural analyses. 100 g of PC was mixed with water, bacterial solution, and calcium lactate as per the mix design and poured in a small plastic vial. After 24 h, the hardened paste sample was removed from the vial, and each sample was stored separately for curing in a small container to avoid contamination. The specimens were cured in fresh tap water for 7 days under ambient laboratory conditions. The average temperature of the lab was 31 ± 2 °C, and relative humidity ranged from 55 to 65% during the curing period. Once the curing period was over, the samples were tested at 7 days, 28 days, and 90 days. Before each microstructural analysis, the samples were oven dried for 2 h at 90 °C to make the sample moisture-free.

Experimental Methods

This study determines different physicochemical parameters for optimal growth of *Bacillus cereus* and the durability enhancements of concrete by inclusions of bacterial solution and calcium lactate. The relationship between mechanical performance and microstructural alterations is investigated as well. The microstructural analyses were performed on the paste samples and presented in detail. Also, the chloride permeability of bacterial concrete specimens was determined using RCPT and water sorptivity tests. The results are compared with the values of traditional PC concrete. Triplicate specimens were used for each test.

Table 3 Concrete mix proportions (Kg/m^3)

Mix ID	Cement	Coarse aggregate (CA)	Fine aggregate (FA)	Water	Calcium lactate	Bacterial solution
PC	400	1032	693	180	–	–
0.5% CL	400	1032	693	180	2	–
1% CL	400	1032	693	180	4	–
1.5% CL	400	1032	693	180	6	–
2% CL	400	1032	693	180	8	–
0.5% BC	400	1032	693	179.1	–	0.9
1% BC	400	1032	693	178.2	–	1.8
1.5% BC	400	1032	693	177.3	–	2.7
2% BC	400	1032	693	176.4	–	3.6
BC + CL	400	1032	693	177.3	6	2.7

The target slump was at least 100 mm for each mix

Compressive Strength Test

Cubic specimens of size 150 mm were used to perform the compressive strength tests. The cubes were compacted using a needle vibrator to achieve uniform compaction. The specimens were demoulded after 24 h and stored in a curing tank for 28 days or till the day of testing. The compressive strength values were determined at ages of 7 days, 28 days, and 90 days. According to ASTM C39/C39M-21 [39] and IS 516 (Part 1/Sec 1): 2021 [40], the compressive strength of concrete was tested using a 3000 kN compression testing machine.

Split Tensile Strength Test

Splitting tensile strength tests were performed on triplicate cylindrical specimens having a diameter of 150 mm and a height of 300 mm for each type of concrete considered in this study. The tests were performed as per IS 5816:1999 [41], equivalent to ASTM C496/C496M-17 [42]. Similar curing and ages of testing were adopted as in the case of compressive strength tests.

Rapid Chloride Permeability Test (RCPT)

To conduct the RCPT, concrete specimens were cast in a cylindrical mould of 100 mm dia and 200 mm height and cured for 28 days. These specimens were tested for 90 days, before starting the test samples are coated with industry-grade epoxy resin and dried up, then a single specimen was cut into three pieces of 100 mm dia and 50 mm thick disc. Two edge discs of thickness 25 mm each were rejected, and the core disc was retained for conducting the RCPT. Then the coated disc specimens were stored in a vacuum desiccator at dry condition for three hours and a further one hour with full submergence in water. The specimens were stored under water for 18 h at atmospheric pressure. Once the sample preparation process was completed, RCPT was conducted on the disc specimen using an operating voltage of 60 V and current was measured at an interval of 30 min for a period of six hours six hours. The charge passed through the concrete was measured in Coulombs from the test. Increasing values of the charge passed indicate increasing permeability of the specimen. The test was performed as per ASTM 1202-22E01 [43]. The average current passed through one cell can be calculated using Eq. (2).

$$Q = 900 \times (I_0 + 2I_{30} + 2I_{90} + 2I_{120} + \cdots + 2I_{300} + 2I_{330} + I_{360}) \quad (2)$$

where Q is the current passed through one cell, I_0 is the current reading soon after the voltage is applied, and I_t is the current at t minutes after initiation of voltage. The results obtained after conducting the test presented in Fig. 12.

Water Sorptivity Test

Water sorptivity tests were conducted as part of this study according to the guidelines of the "Durability Index Testing Procedure Manual ver 4.5.1, April (2018)" [44] published by the University of the Witwatersrand, Johannesburg as suggested by existing literature [45–47]. For this test, a central core with a diameter of 70 mm was obtained from a 150 mm concrete cube with an age of 28 days using a core cutting machine. This cylindrical core was dried and then coated with epoxy resin. After drying the coated core sample, it was cut into four equal pieces, each having a diameter of 70 mm and a height of 30 mm. These cut samples were then stored in a hot air oven at a temperature of 50 ± 2 °C for 7 days. Subsequently, these samples were taken out and stored in a desiccator at a temperature of 23 ± 2 °C for 2 h. Then the dimensions of each sample were measured using a vernier caliper. Then saturated calcium hydroxide solution was poured into a tray, and samples were placed as shown in Fig. 2. Following this, the weight of each sample was recorded after 3, 5, 7, 9, 12, 16, 20, and 25 min, respectively. Then the samples were stored at a vacuum of between − 75 and − 80 kPa for 3 h ± 15 min in dry conditions, followed by complete immersion in saturated calcium hydroxide solution for 1 h ± 15 min. Then the samples were taken out of the vacuum and soaked in the saturated calcium hydroxide solution for a further 18 ± 1 h. Finally, the saturated mass was recorded for each sample, and the water sorptivity was calculated as per the series of equations provided by "Durability Index Testing Procedure Manual ver 4.5.1, April (2018)" [44]. The corresponding results are presented in Fig. 2.

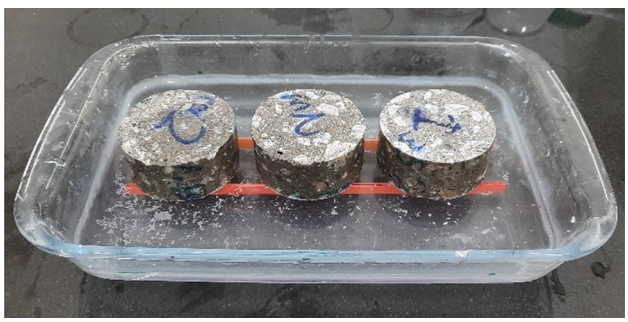

Fig. 2 Samples for water sorptivity testing stored in saturated calcium hydroxide solution

Microstructural Analyses

Scanning Electron Microscopy (SEM)

The changes in morphology and the corresponding elemental compositions were investigated using a scanning electron microscope. A SEM setup was used to capture micrographs at a working distance of 10 mm using an Everhart Thornley detector (ETD) at a magnification of 2500× and 10,000× at an operating voltage of 10 kV. Crushed particles of approximately 2 mm^2 area obtained from hardened cement paste samples with smooth surfaces were used for these analyses. Each sample was oven-dried for 2 h to ensure to remove any free moisture prior to the SEM analysis. Using a standard desktop sputter coater, the samples were subsequently coated with a silver layer of 10 nm thickness to make them conductive and obtain high-resolution micrographs. The specimens were then placed in metal stubs with carbon tape to prevent them from getting displaced. The micrographs were captured under vacuum at a pressure of 9.95×10^{-5} Pa. The corresponding results are presented in Figs. 14, 15 and 16.

X-Ray Photoelectron Spectroscopy (XPS)

To detect the presence of elements and their chemical state within a material or covering its surface, X-ray photoelectron spectroscopy (XPS) was performed. Thermo-Fisher Avantage software was used to analyse the elements present in the powdered samples. The corresponding results are presented in Fig. 17.

X-Ray Diffraction Analysis (XRD)

Hardened cementitious paste samples were crushed into powdered form for the XRD analyses. CuKα X-rays operating at 30 mA current and 40 kV operating voltage with a scan speed of 2°/min were used for the analyses. A step width of 0.02° across a 2θ range of 5° to 90° was used for the assessment as per the suggestions from existing literature [48]. The diffractograms were analyzed using PANalytical X'Pert HighScore software and presented in Fig. 18.

Fourier Transform Infrared Spectroscopy (FTIR)

Fourier transform infrared spectroscopy (FTIR) analyses were performed to determine the differences in molecular bonds and the accompanying vibrations were recorded for the same samples used for the XRD analyses. The KBr pellet arrangement was used to prepare the samples for FTIR analyses. Each analysis was performed in the mid-infrared range having wave numbers between 4000 and 400 cm^{-1} with at an interval of 4 cm^{-1}. The molecular bonds pertaining to distinct molecular vibrations were recorded in the transmission mode. The results obtained are presented in Fig. 19.

The results and discussions for the experiments mentioned above are presented in the next section.

Results

Optimization of Bacterial Growth

From Fig. 3, it was found that the growth of *Bacillus cereus* is maximum when growth inoculated with 1.5% of culture media containing 10^7 to 10^{11} cells/mL of primary culture. Although the optical density is almost the same for all variations, the cell/mL is significantly different. The increase in OD of 1.5% IV is nearly 6.50% and 4.85% compared to 1% IV and 2% IV, respectively, hence 1.5% IV taken as optimum inoculum volume for bacterial growth.

Similarly, from Fig. 4, SV20 was optimum for growing *Bacillus cereus* in broth containing 20 g of LB Miller. It is evident from Fig. 4 that SV25 results in more growth than SV20, but SV20 is selected as the optimum to reduce the cost of bacterial production, as the difference of OD is not more than 1%.

Furthermore, from Fig. 4, pH of 7 was optimum as the growth of *Bacillus cereus* is maximum, and the growth curve is prominent. From Fig. 5, it is evident that *Bacillus cereus* can grow at high alkaline medium having pH value of 9, although the OD dropped by approximately 16% compared to a medium with pH of 7.

Compressive Strength

The optimization of CL and BC dosages is obtained by comparing compressive strength between concrete with bacterial inclusions and PC concrete. The compressive strength is found to increase for all the variations of calcium lactate w.r.t. the M40 grade PC concrete mix, as evident from Fig. 6.

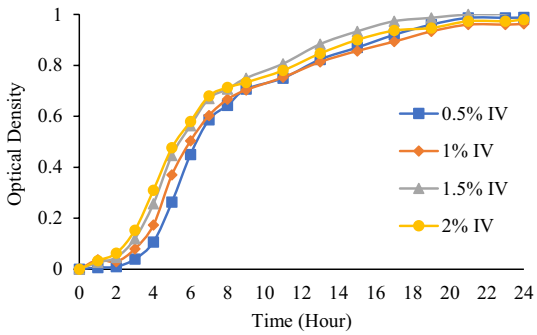

Fig. 3 Inoculum volume optimization for *Bacillus cereus*

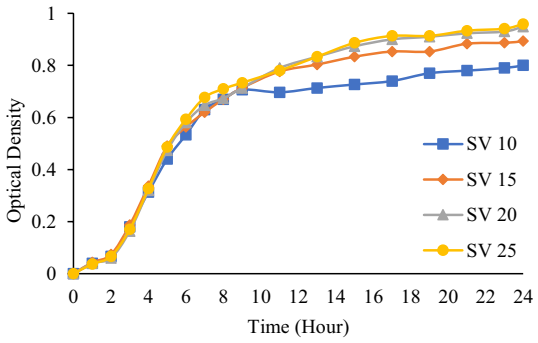

Fig. 4 Substrate volume optimization for *Bacillus cereus*

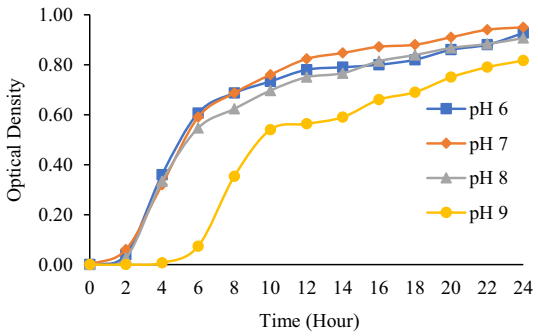

Fig. 5 pH value optimization for *Bacillus cereus*

It is also observed that the percentage increase in compressive strength using calcium lactate is approximately 16% to 22% after 7 days curing, 6% to 13% after 28 days, and 15% to 26% after 90 days. Similar observation was reported in previous study on concrete containing 0.5% CL [48]. After comparing all four variations, it was found that till 1.5% CL strength increases w.r.t M40 PC concrete for 7 days, 28 days, and 90 days which is about 22%, 13%, and 26%, respectively. These findings are consistent with the results reported in existing literature [49]. The addition of 2% CL decreases strength, approximately 2% w.r.t to 1.5% CL. Hence, 1.5% CL was an optimum dose of calcium lactate from the above observations.

A similar approach is adopted for BC optimization, as shown in Fig. 7. It is observed that the compressive strength of concrete incorporated with *Bacillus cereus* with varying percentages w.r.t water content is increasing significantly. Four different percentages viz. 0.5%, 1%, 1.5% and 2% w.r.t water content of M40 mix PC concrete accounts for increase in strength from 8–16%, 4–10%, and 18–24% for 7 days, 28 days and 90 days concrete, respectively. It was found that 1% of *Bacillus cereus* full-grown culture media is optimum as it gives maximum strength w.r.t to PC, 0.5%, 1.5%, and 2% BC. The compressive strength of 1% BC increases about 24% for 90 days of concrete compared to M40 grade PC, which is maximum among all four variations. Hence, the optimum quantity of bacterial solution is 1% w.r.t. water content.

Thus, the optimal proportions of CL and BC, respectively, are found to be 1.5% and 1%. The compressive strength results of the mix prepared with this optimum BC + CL combination are presented in Fig. 8a. It is observed that the strength is significantly increasing w.r.t. M40 grade PC by 14%, 14%, and 18% for 7 days, 28 days, and 90 days, respectively. Furthermore, the BC + CL increases strength w.r.t PC, optimum BC, and optimum CL for 28 days but decreases w.r.t optimum BC and optimum CL for 90 days by 8% and 13%, respectively. The target slump of 100 mm to be attained by the optimal BC + CL as presented in Fig. 8b.

Splitting Tensile Strength

The splitting tensile strength of each of the CL mixes increases w.r.t. the PC concrete mix (Fig. 9). The increase in splitting tensile strength is approximately 2–6%, 3–7%,

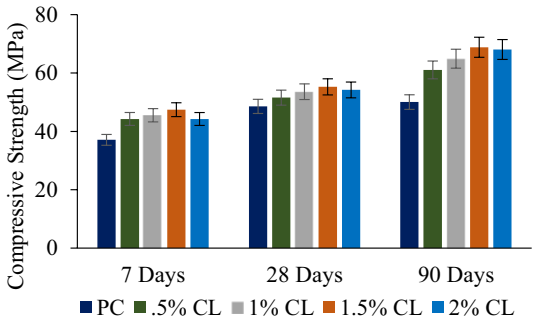

Fig. 6 Comparison of concrete compressive strength values of different CL mixes w.r.t. PC

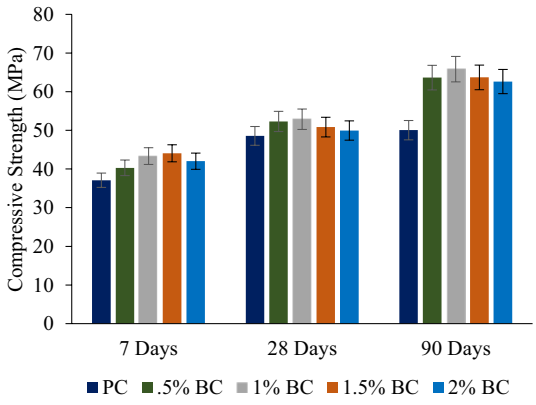

Fig. 7 Comparison of concrete compressive strength values of different BC mixes w.r.t PC

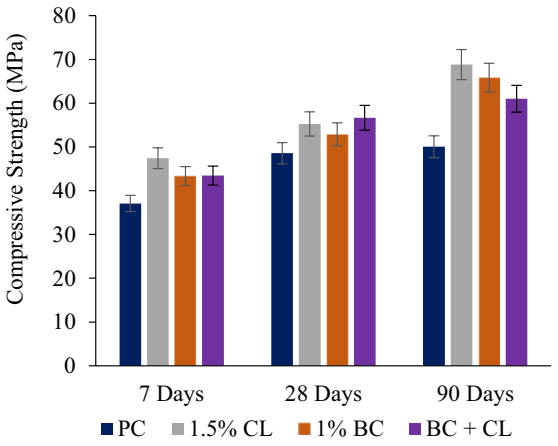

(a)

(b)

Fig. 8 **a** Comparison of concrete compressive strength values of optimal CL, BC, and BC + CL mixes w.r.t PC. **b** Slump height of optimal BC + CL mix

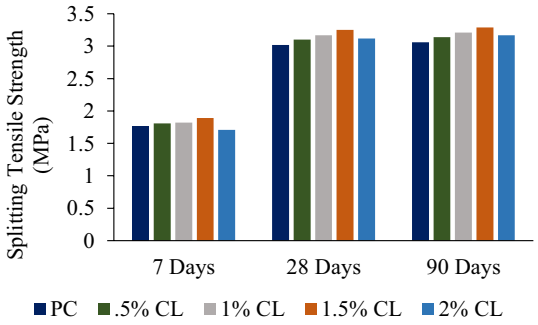

Fig. 9 Comparison of concrete splitting tensile strength values of different BC mixes w.r.t PC

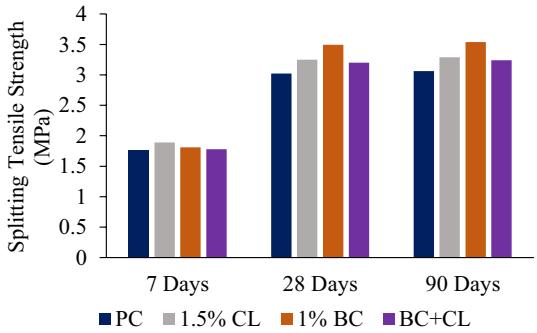

Fig. 11 Comparison of concrete splitting tensile strength values of optimal CL, BC, and BC + CL mixes w.r.t PC

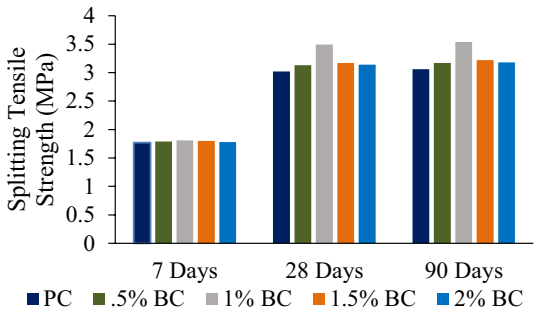

Fig. 10 Comparison of concrete splitting tensile strength values of different BC mixes w.r.t PC

and 2–7% after 7 days, 28 days, and 90 days, respectively. As in the case of compressive strength, the maximum splitting tensile strength values are observed in the case of 1.5% CL mixes (Fig. 9). The increase in the values of splitting tensile strength due to bacterial inclusions are attributed to the densification of microstructure and bio-mineralization due to MICP in the interfacial transition zone (ITZ). These observaions are validated through SEM (Figs. 14, 15, 16b–d) and FTIR spectroscopy (Fig. 19).

For bacterial inclusions in concrete, the increase in splitting tensile strength w.r.t. PC concrete is observed to be less than 1% at the age of 7 days (Fig. 10). The corresponding increase at the ages of 28 and 90 days is in the range of 3–7% and 3–6%, respectively. As shown in Fig. 10, the maximum increase in splitting tensile strength due to bacterial inclusions w.r.t. PC concrete is observed for 1% BC mixes at ages of both 28 days (7%) and 90 days (6%). As reported earlier, the maximum increase in compressive strength due to bacterial inclusions is also observed in the case of the 1% BC mixes at all ages.

The above discussion shows the maximum splitting tensile strength for the 1.5% CL and 1% BC mixes. The corresponding results for the BC + CL mixes prepared with these optimal combinations of CL and BC are presented in Fig. 11. It is observed that the increase in splitting tensile strength w.r.t. PC is 0.5%, 6%, and 5% for 7 days, 28 days, and 90 days, respectively. However, there is an observed

reduction of approximately 2% w.r.t. the 1.5% CL and 1% BC mixes at all ages.

It is observed that the increase in the values of compressive and splitting tensile strength are different in the case of bacterial concrete compared to traditional PC concrete. The formation of calcite during MICP and the presence of unreacted calcium lactate and the bacterial cells in the microstructure modify the morphology of the hardened cementitious paste. Even if the pores are filled with MICP leading to the increase in compressive strength, the presence of unreacted calcium lactate and the brittle calcite in the ITZ can actually prevent the formation of a homogenous matrix, thereby slightly reducing the tensile strength. Hence, the observed increase in tensile strength is not as prominent as the corresponding increase in compressive strength of bacterial concrete. Consequently, the strength development in bacterial concrete does not exhibit the same trend as its PC concrete counterpart. The findings from the microstructural analyses are presented in Sect. 4.6 to corroborate these observations.

RCPT

RCPT results show that the charge passed for 0.5% BC is the lowest compared to all the other concrete mixes with bacterial inclusions. It is also observed that 0.5% CL experiences the lowest charge passed among all the mixes with CL additions to concrete. According to ASTM C1202-22E01, Table X1.1 [43], most of the concrete mixes can be categorized as exhibiting moderate chloride permeability. However, the 2% CL and BC + CL mixes evince high chloride permeability. Figure 12 also shows that the increase in CL content to 1.5% reduces chloride permeability w.r.t. the control PC mix, whereas the addition of 2% CL makes the concrete more susceptible to chloride ion penetration.

Similarly, the bacterial inclusions reduce the permeability, but an increase in bacterial quantity also increases the permeability. It is observed from Fig. 8 that 0.5% BC has less permeability of 18.27% than 2% BC. For BC + CL, it was observed that the chloride permeability rises significantly as the precipitation of $CaCO_3$ is seen in large quantities in both monoclinic and hexagonal forms (Fig. 14d). During $CaCO_3$ formation, a large number of Ca^{2+} ions remain unreacted and accumulate outside the bacterial cells. The presence of Ca^{2+} ions in bacterial concrete has been reported in previous studies [25, 49, 51–53]. This accumulated Ca^{2+} accelerates the penetration of chloride ions, resulting in increased permeability. The results will be correlated with microstructure analysis.

Water sorptivity was evaluated as an additional parameter to confirm the reduction in water permeability due to bacterial inclusions. The results of the water sorptivity test for all mixes at 28 days are presented in the next section.

Water Sorptivity Test

It can be observed from Fig. 13 that the PC concrete mix shows high water sorptivity compared to the CL and BC mixes after 28 days of water curing. From Fig. 13, it is evident that the increase in the proportions of CL and BC leads to a decrease in water sorptivity. The reduction in water sorptivity index w.r.t. the PC concrete mix for the CL mixes varies from 8 to 37%, and for the BC mixes from 2 to 13%. It is observed that the BC + CL mix exhibits a reduction of 55% w.r.t. the PC mix, which is the maximum among all the mixes. This observation is attributed to the coexistence of calcium lactate, the bacterial cells, and the different forms of calcite along with the hardened cementitious paste, as confirmed through microanalyses.

The observations from water sorptivity assessments demonstrate that the addition of bacterial cells along with suitable nutrients enhances the resistance of concrete towards the ingress of water.

In the next section, the observations from the compressive strength, splitting tensile strength, RCPT and water sorptivity are correlated with the corresponding changes in the

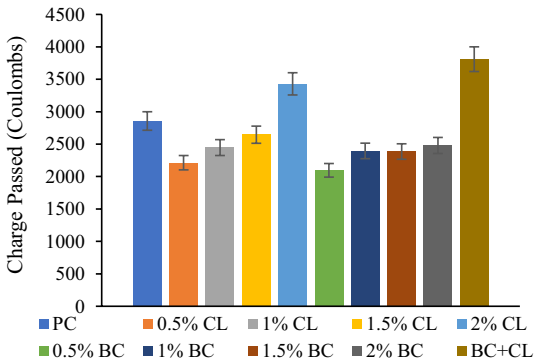

Fig. 12 RCPT results at 90 days for all concrete mixes

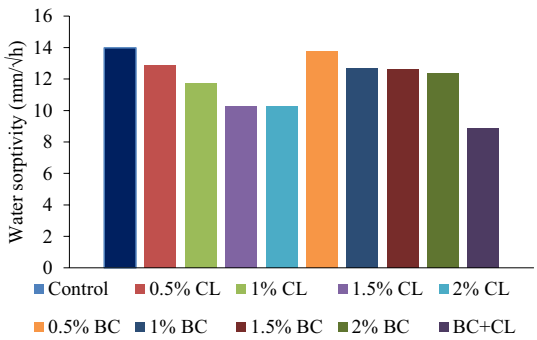

Fig. 13 Water sorptivity results at 28 days for all concrete mixes

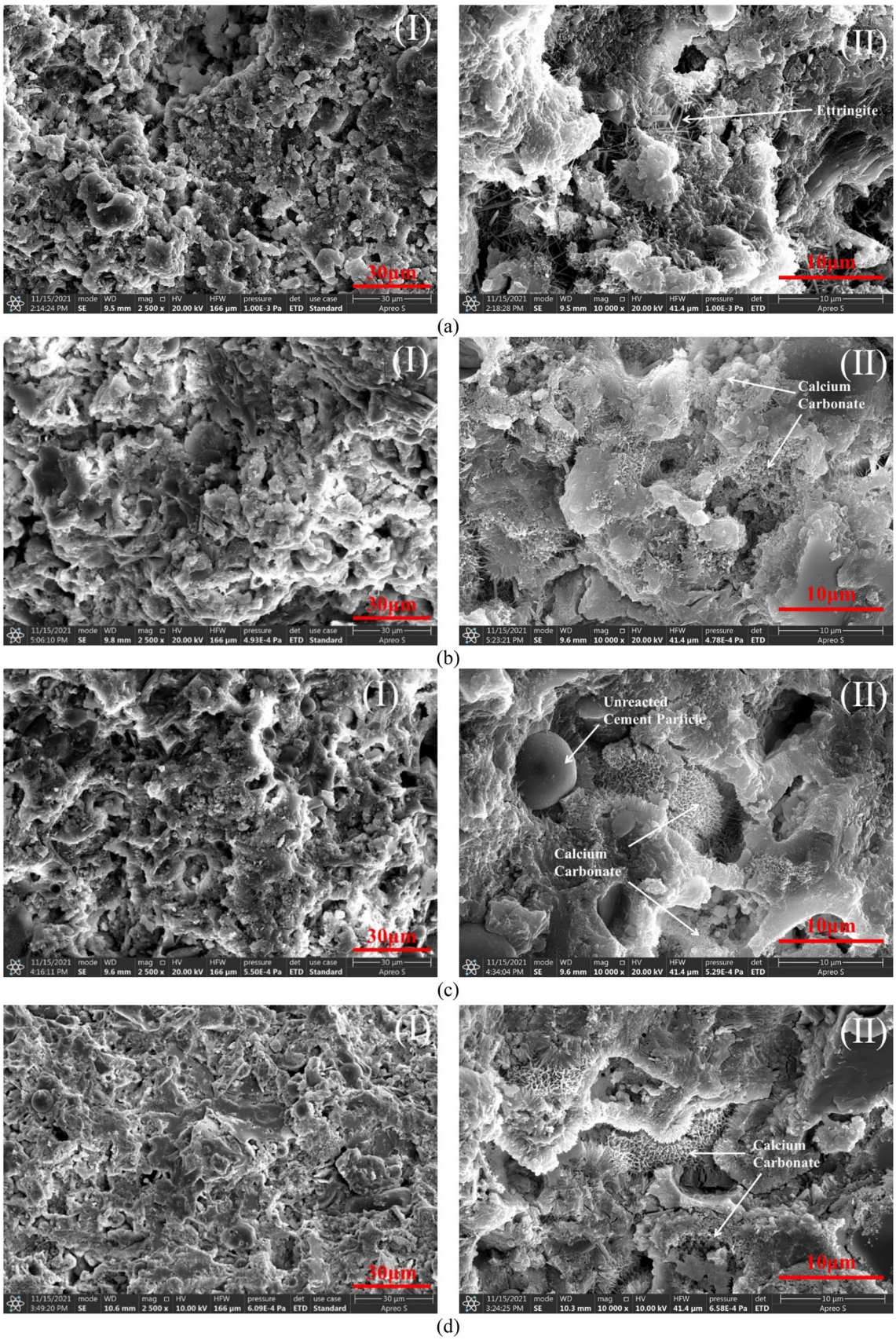

Fig. 14 Micrographs of 7 days **a** PC, **b** 1% BC, **c** 1.5% CL, **d** BC + CL (I—2500 × II—10,000 × magnification)

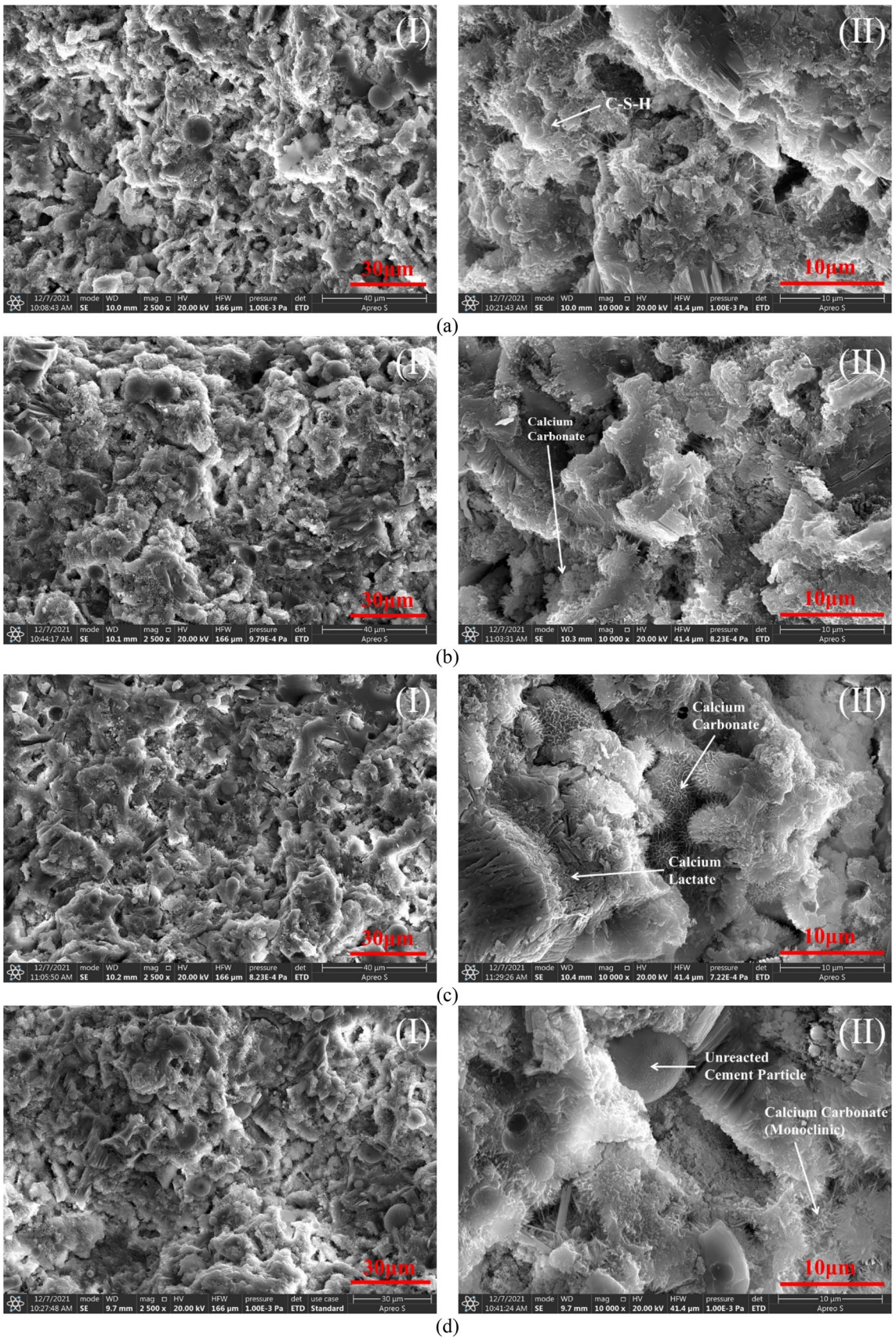

Fig. 15 Micrographs of 28 days **a** PC, **b** 1% BC, **c** 1.5% CL, **d** BC + CL (I—2500×, II—10,000× magnification)

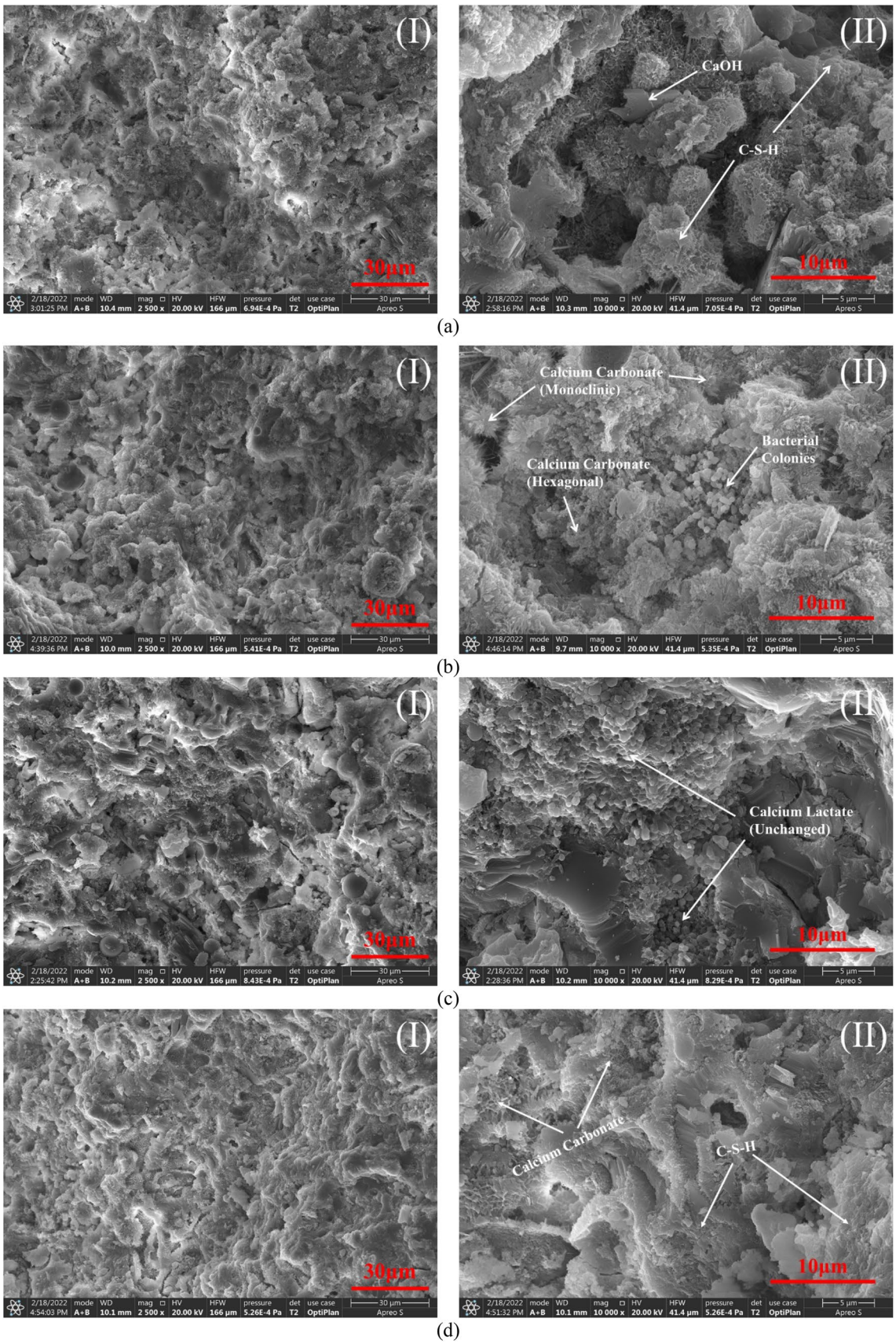

Fig. 16 Micrographs of 90 days **a** Control PC, **b** 1% BC, **c** 1.5% CL, **d** BC + CL (I—2500×; III—10,000× magnification)

microstructure of hardened PC pastes with the aforementioned additions of CL, BC, and BC + CL.

Microstructural Analyses

Figures 14, 15 and 16 present the micrographs obtained from SEM analyses conducted on hardened paste samples having ages of 7, 28, and 90 days. For each age, the micrographs are captured at magnifications of 2500× and 10,000×. From Fig. 14a, the formation of ettringite is clearly visible in case of PC at age of 7 days. From Fig. 14b, it is observed that the presence of unreacted cement particles is present as the formation of calcite forming an outer layer over the cement surface. Also, for 1.5% CL the bouquets-needle-like formation of calcite was observed. Also, from Fig. 14c, it was seen that at early age, the morphology of 1% BC is completely different from that of PC. The formation of long slender prismatic needles of ettringite was visible to a slight extent in the case of hardened BC paste. This observation is due to the presence of calcite in monoclinic form. These calcite formations lead to the development of coating over the ettringite crystals, leading to the development of the bouquets-needle like morphology. These findings match the observation from a previous study [21].

From Fig. 15a, it is observed that the morphology of PC changed from 7 days sample due to the formation of newer microstructural phases. The conversion of ettringite and portlandite into a C–S–H matrix is visible, and a homogeneous morphology is seen. For 1.5% CL (Fig. 15b), it is observed that unreacted residue of calcium lactate and the formation of hexagonal $CaCO_3$ coexist. Similarly, for 1% BC samples (Fig. 15c), unreacted PC residue is significantly reduced, and the formation of $CaCO_3$ is seen in bouquet-needle-like morphology. For BC + CL mixes (Fig. 15d), unreacted PC residue is present in negligible content, and the formation of $CaCO_3$ is visible in both monoclinic and hexagonal forms. It is also observed that pores in the sample are filled with MICP, and a homogeneous morphology is seen. The formations of additional chemical phases lead to the thickening of the ITZ and densification of the microstructure. These findings are consistent with those of existing studies [53].

Micrographs at 90 days (Fig. 16) show significant microstructural changes compared to the earlier ages. These changes can be correlated to the trends observed in the mechanical strength values, RCPT results, and water sorptivity results. The control PC mix exhibited a greater proportion of pores than 1% BC, 1.5% CL, and BC + CL, leading to lesser mechanical strength than the bacterial concrete mixes. At 10,000× magnification, it can be seen that the pores and voids are filled with MICP in the case of 1% BC, 1.5% CL, and BC + CL mixes. Similar observation is seen in previous studies [25, 50, 54]. From Fig. 16b, 1% BC showed MICP in pores near the locations of the bacterial cells. Also, the formations of $CaCO_3$ crystals at higher magnification were observed. The pores filled with MICP increase the strength of the concrete and decrease chloride permeability and water sorptivity. As seen earlier, the increase in calcium lactate content up to 1.5% increases the strength and reduces the chloride permeability. Further increase in calcium lactate content beyond 1.5% results in a decrease in strength and an increase in chloride permeability. The densification of microstructure and the bio-mineralization in the ITZ are attributed to the observed changes in mechanical and chemical characteristics of the concrete specimens.

From Fig. 16c, it can be seen that the calcium lactate is in an unchanged state in the case of 1.5% CL mixes. This calcium lactate fills the pores, increasing the compressive strength. However, it increases the chloride permeability as the conversion to $CaCO_3$ cannot occur without *Bacillus cereus* inclusions. As a result, in the case of BC + CL (Fig. 16d), the combined presence of calcium lactate and *Bacillus cereus* inclusions leads to the formation of MICP. Additionally, unreacted calcium lactate was observed to a lesser extent.

In contrast to 28 days samples, unreacted PC residue was absent in the 90-day samples of the 1% BC, 1.5% CL, and BC + CL mixes. As a result, an increase in compressive and splitting tensile strength values with age were observed for the 90-d specimens (Figs. 8a and 11). These morphological changes are also attributed to the changes in water sorptivity characteristics due to bacterial inclusions and consequent MICP in concrete.

As mentioned earlier, XPS analyses were conducted to correlate the morphological changes observed from SEM with the changes in atomic percentage and the binding

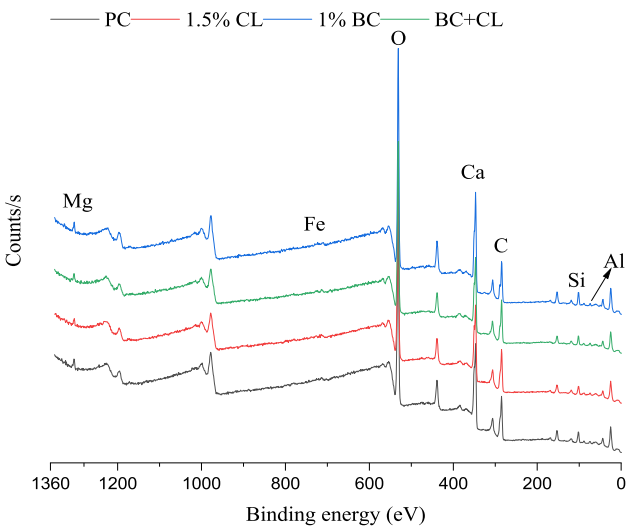

Fig. 17 XPS spectrum of optimum PC, 1% BC, 1.5% CL and BC + CL mixes

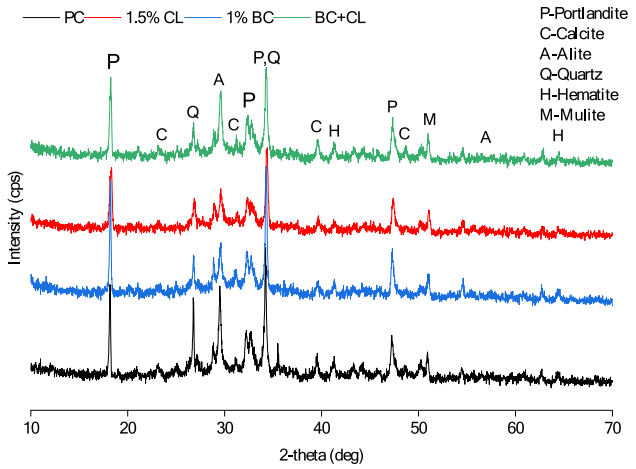

Fig. 18 XRD patterns of PC, 1% BC, 1.5% CL and BC + CL samples

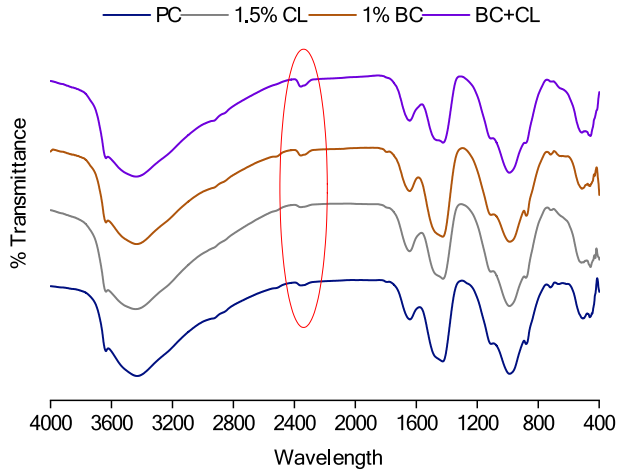

Fig. 19 FTIR spectra of optimum PC, 1% BC, 1.5% CL and BC + CL

energy (eV) caused by the conversion of calcium lactate to $CaCO_3$ during MICP. To conduct XPS, XRD, and FTIR analyses, 90-day samples were selected as the precipitation due to the addition of bacteria and calcium lactate were prominent in the microstructure, compared to the 7-day and 28-day samples. From Fig. 17, the presence of Ca, O, C, Si, Al, Fe, Mg were confirmed along with their respective atomic percentages. Also, the changes in binding energy due to the incorporation of bacteria and calcium lactate were obtained and correlated with the results of RCPT. The combined increase in atomic percentages of Ca, O, and C combined is the maximum for 1% BC and 1.5% BC to the tune of approximately 2% w.r.t PC.

Additionally, mineralogical analyses were conducted to confirm calcite formation during MICP from the diffractograms in Fig. 18. The peaks corresponding to portlandite (P), calcite (C), alite (A), quartz (Q), hematite (H), and mullite (M) were observed. It was observed that the calcite crystals existed in two different forms: monoclinic and hexagonal, as visible from the micrographs (Fig. 16b-II). $CaCO_3$ was present in PC and 1.5% CL in the form of monoclinic crystals, but hexagonal crystals were observed for 1% BC and BC + CL. This observation is consistent with the findings from SEM (Figs. 15b-II and 16b-II). $CaCO_3$ in both forms was present in BC + CL in significant quantities, leading to increased chloride permeability. As mentioned earlier, the unreacted Ca^{2+} ions from bacterial metabolic activities accelerate the chloride ion penetration by forming $CaCl_2$ during the RCPT analysis. The presence of these Ca^{2+} ions is confirmed by the change in binding energy observed in Fig. 17.

The formation of new chemical bonds and molecular vibrations are presented in Fig. 19 as obtained through FTIR spectroscopy. The formation of the O=C=O stretching bond at a wave number near 2350 cm^{-1} was prominent in each of the BC and BC + CL mixes. For PC and 1.5% CL, the presence of O=C=O bond is undetected. This O=C=O bond, in the case of 1% BC and BC + CL, confirms the presence of $CaCO_3$ crystals indicated by the XRD and SEM analyses. The observations from this study agree with previous findings [55]. The effects of these chemical bonds were visible in the trends of compressive strength values (Fig. 8), splitting tensile strength (Fig. 11), RCPT results (Fig. 12), and water sorptivity results (Fig. 13).

The observations from the mechanical and chemical evaluations are correlated with the findings from mineralogical, molecular, and microstructural analyses.

Practical and Economic Aspects of Bacterial Concrete

It is worth mentioning here that the inclusions of bacterial solutions in concrete require skilled personnel. Hence, the field workers and relevant personnel have to be provided with the necessary training and practice for the preparation of bacterial culture and their incorporation in concrete. One of the possible approaches to ease the associated complexities is to add the bacterial strains in dry powdered form along with the dry ingredients of cement concrete and to add the requisite quantities of water and nutrients as per the requirements of workability, strength, and durability.

Another critical parameter to be considered for the widespread usage of bacterial concrete is the economic aspect. Based on the cost of locally available materials in Hyderabad and the bacterial strains obtained from the central agencies, it is estimated that the unit cost of the optimal BC + CL mix used in this study is approximately INR 5000 per m^3. Compared to conventional PC concrete, thus this mix is around 21% more expensive if only the cost of production is considered. However, the primary benefit of

bacterial inclusions in concrete is to eliminate the need for regular maintenance and repair due to the self-healing characteristics that repair the cracks in concrete. Additionally, the need for the materials used for these repair activities are also eliminated. Hence, to fully comprehend the benefits of bacterial concrete, life cycle assessments shall be conducted in the future as an extension of this study.

Conclusions

Based on the present study, the following conclusions can be drawn.

1. The optimal physicochemical parameters for the growth of *Bacillus cereus* are: inoculum volume of 1%; Miller LB broth quantity of 20 gm per 1000 mL of distilled water as substrate; and a pH value of 7.
2. *Bacillus cereus* is also found to grow at a pH value of 9 and above, showing its compatibility with the high pH environment present in concrete.
3. Addition of 1% solution of *Bacillus cereus* in PC concrete resulted in a 14.42%, 8.15%, and 23.98% increase in compressive strength after 7 days, 28 days, and 90 days, respectively. It is also observed that the increase in bacterial dosage beyond 1% leads to decreasing compressive strength w.r.t. the 1% BC mixes. It is observed that the strength gain for 2% BC mixes is 11.71%, 2.78% and 20.09% after 7 days, 28 days and 90 days, respectively, which is less compared to 1% BC inclusions. It is observed that the BC + CL mix with 1% BC and 1.5% CL exhibits the maximum compressive strength values at each age.
4. It is observed that the increase in splitting tensile strength values of the BC + CL mix w.r.t. PC is 0.5%, 6%, and 5% for 7 days, 28 days, and 90 days, respectively.
5. It is observed that 0.5% BC shows a reduction of 26.2% in chloride permeability w.r.t. PC mixes. The corresponding reduction for 1% and 2% BC are observed as 19.25% and 15.2%, respectively. In case of calcium lactate addition, 0.5% CL mixes exhibit nearly 29% reduction in chloride permeability. However, CL addition beyond 1.5% increases the chloride permeability w.r.t. PC mix. This increase is nearly 16% in case of 2% CL addition.
6. It is found that the water sorptivity of BC + CL shows 57% reduction as compared to PC mixes.
7. Microstructural analyses provide conclusive evidence of MICP, which increases the compressive strength and reduces the chloride permeability.
8. Hence, this study recommends 1% BC addition as the optimal one for concrete mixes from the aspect of mechanical strength as well as resistance to chloride and water ingress. 1% BC resulted in a 14.42%, 8.15%, and 23.98% increase in compressive strength and 3%, 13%, and 12% increase in split tensile strength after 7 days, 28 days, and 90 days, respectively, compared to PC. Also, the chloride permeability and water sorptivity reduction are 19.25% and 10.25%, respectively, w.r.t PC concrete. Further investigations on mechanical, chemical, and life cycle aspects are necessary to provide standardized recommendations for the inclusion of bacterial strains in concrete applications.

Acknowledgements The authors are grateful to the Central Analytical Laboratory at BITS-Pilani, Hyderabad Campus, for providing the adequate setup to perform XRD, XPS, FTIR, and SEM analyses. Also, the authors would like to acknowledge the Department of Biology, BITS-Pilani, Hyderabad campus, for providing the resources to conduct initial experiments related to the study.

Funding This study is sponsored by the Council of Scientific and Industrial Research (CSIR), Ministry of Science of Technology, Govt. of India, EMR-II Scheme, Project No. 22/0770/18.

Declarations

Conflicts of interest The authors declare no conflict of interest.

References

1. M. Garside, Major countries in worldwide cement production 2010–2020, Statista (2021)
2. Statista, Global investments on the construction and maintenance of infrastructure as share of GDP in 2019, by country (2019). https://www.statista.com/statistics/566787/average-yearly-expenditure-on-economic-infrastructure-as-percent-of-gdp-worldwide-by-country/. Accessed 10 March 2022
3. R.M. Andrew, Global CO_2 emissions from cement production, 1928–2018. Earth Syst. Sci. Data **11**, 1675–1710 (2019). https://doi.org/10.5281/zenodo.831454
4. Ministy of Power Bureau of Energy Efficiency, Government of India, Cement (2021). https://beeindia.gov.in/node/166. Accessed 8 Feb 8 2021
5. J.Y. Wang, N. De Belie, W. Verstraete, Diatomaceous earth as a protective vehicle for bacteria applied for self-healing concrete. J. Ind. Microbiol. Biotechnol. **39**, 567–577 (2012). https://doi.org/10.1007/s10295-011-1037-1
6. P.K. Mehta, P.J.M. Monteiro, *Concrete: Microstructure, Properties, and Materials*, 4th edn. (McGraw-Hill Education, New York, 2014)
7. H.M. Jonkers, A. Thijssen, G. Muyzer, O. Copuroglu, E. Schlangen, Application of bacteria as self-healing agent for the development of sustainable concrete. Ecol. Eng. **36**, 230–235 (2010). https://doi.org/10.1016/j.ecoleng.2008.12.036
8. H.M. Jonkers, E. Schlangen, A two component bacteria-based self-healing concrete, in *Proceedings Second International*

Conference on Concrete Repair, Rehabilitation and Retrofitting (2008), pp. 119–120
9. P. Ghosh, S. Mandal, B.D. Chattopadhyay, S. Pal, Use of microorganism to improve the strength of cement mortar. Cem. Concr. Res. **35**, 1980–1983 (2005). https://doi.org/10.1016/j.cemconres.2005.03.005
10. H.M. Jonkers, Bacteria-based self-healing concrete. Heron **56**(1/2), 1–12 (2011)
11. S. Majumdar, M. Sarkar, T. Chowdhury, B. Chattopadhyay, S. Mandal, Use of bacterial protein powder in commercial fly ash pozzolana cements for high performance construction materials. Open J. Civ. Eng. **02**, 218–228 (2012). https://doi.org/10.4236/ojce.2012.24029
12. M.S. Vekariya, J. Pitroda, Bacterial concrete: new era for construction industry. Int. J. Eng. Trends Technol. **4**(9), 4128–4137 (2013)
13. M.V.S. Rao, V.S. Reddy, M. Hafsa, P. Veena, P. Anusha, Bio-engineered concrete—a sustainable self-healing construction material (2013). www.isca.in
14. N. Chahal, R. Siddique, A. Rajor, Influence of bacteria on the compressive strength, water absorption and rapid chloride permeability of concrete incorporating silica fume. Constr. Build. Mater. **37**, 645–651 (2012). https://doi.org/10.1016/j.conbuildmat.2012.07.029
15. W. De Muynck, D. Debrouwer, N. De Belie, W. Verstraete, Bacterial carbonate precipitation improves the durability of cementitious materials. Cem. Concr. Res. **38**, 1005–1014 (2008). https://doi.org/10.1016/j.cemconres.2008.03.005
16. S. Mindess, F.J. Young, D. Darwin, Concrete 2nd edn., Techn Doc. (2003).
17. R. Siddique, N.K. Chahal, Effect of ureolytic bacteria on concrete properties. Constr. Build. Mater. **25**, 3791–3801 (2011). https://doi.org/10.1016/j.conbuildmat.2011.04.010
18. S.K. Ramachandran, V. Ramakrishnan, S.S. Bang, Remediation of concrete using microorganisms. ACI Mater. J. (2001). https://doi.org/10.14359/10154
19. K. Vijay, M. Murmu, S.V. Deo, Bacteria based self healing concrete—a review. Constr. Build. Mater. **152**, 1008–1014 (2017). https://doi.org/10.1016/j.conbuildmat.2017.07.040
20. E. Stanaszek-Tomal, Bacterial concrete as a sustainable building material? Sustainability **12**, 1–13 (2020). https://doi.org/10.3390/su12020696
21. T.H. Nguyen, E. Ghorbel, H. Fares, A. Cousture, Bacterial self-healing of concrete and durability assessment. Cem. Concr. Compos. **104**, 1–49 (2019). https://doi.org/10.1016/j.cemconcomp.2019.103340
22. S. Ghosh, M. Biswas, B.D. Chattopadhyay, S. Mandal, Microbial activity on the microstructure of bacteria modified mortar. Cem. Concr. Compos. **31**, 93–98 (2009). https://doi.org/10.1016/j.cemconcomp.2009.01.001
23. J.Y. Wang, H. Soens, W. Verstraete, N. De Belie, Self-healing concrete by use of microencapsulated bacterial spores. Cem. Concr. Res. **56**, 139–152 (2014). https://doi.org/10.1016/j.cemconres.2013.11.009
24. R. Siddique, A. Jameel, M. Singh, D. Barnat-Hunek, A. Kunal, R. Aït-Mokhtar, A.R. Belarbi, Effect of bacteria on strength, permeation characteristics and micro-structure of silica fume concrete. Constr. Build. Mater. **142**, 92–100 (2017). https://doi.org/10.1016/j.conbuildmat.2017.03.057
25. Q. Chunxiang, W. Jianyun, W. Ruixing, C. Liang, Corrosion protection of cement-based building materials by surface deposition of CaCO3 by *Bacillus pasteurii*. Mater. Sci. Eng. C. **29**, 1273–1280 (2009). https://doi.org/10.1016/j.msec.2008.10.025
26. K.K. Sahoo, A.K. Sathyan, C. Kumari, P. Sarkar, R. Davis, Investigation of cement mortar incorporating *Bacillus sphaericus*. Int. J. Smart Nano Mater. **7**, 91–105 (2016). https://doi.org/10.1080/19475411.2016.1205157
27. M. Luo, C.X. Qian, R.Y. Li, Factors affecting crack repairing capacity of bacteria-based self-healing concrete. Constr. Build. Mater. **87**, 1–7 (2015). https://doi.org/10.1016/j.conbuildmat.2015.03.117
28. V. Achal, A. Mukherjee, M.S. Reddy, Microbial concrete: a way to enhance durability of building structures, in: *2nd International Conference on Sustainable Construction Materials and Technologies* (2010), pp. 23–28. https://doi.org/10.1061/(asce)mt.1943-5533.0000159
29. N. De Belie, E. Gruyaert, A. Al-Tabbaa, P. Antonaci, C. Baera, D. Bajare, A. Darquennes, R. Davies, L. Ferrara, T. Jefferson, C. Litina, B. Miljevic, A. Otlewska, J. Ranogajec, M. Roig-Flores, K. Paine, P. Lukowski, P. Serna, J.M. Tulliani, S. Vucetic, J. Wang, H.M. Jonkers, A review of self-healing concrete for damage management of structures. Adv. Mater. Interfaces. **5**, 1–28 (2018). https://doi.org/10.1002/admi.201800074
30. Bureau of Indian Standard (BIS), Ordinary Portland Cement—Specifications, IS 269:2015
31. ASTM C150-21 (Standard Specification for Portland Cement), 2021 Annual Book of ASTM Standards, Vol. 04.01, Cement; Lime; Gypsum, American Society for Testing and Materials
32. Bureau of Indian Standard (BIS), Coarse and fine aggregate for concrete—Specification, IS 383 (2016)
33. ASTM C33/C33M-18 (Standard Specification for Concrete Aggregates), 2021 Annual Book of ASTM Standards, Vol. 04.02, Concrete and Aggregates, American Society for Testing and Materials
34. F.A. Drobniewski, *Bacillus cereus* and related species. Clin. Microbiol. Rev. **6**, 324–338 (1993). https://doi.org/10.1128/CMR.6.4.324
35. A.C. Smith, M.A. Hussey, Gram stain protocols. Am. Soc. Microbiol. **1**, 1–9 (2016)
36. D.K. Maheshwari, *Practical Microbiology* (S. Chand Publishing, New Delhi, 2002)
37. D.E. Dixon, J.R. Prestrera, G.R. Burg, S.A. Chairman, E.A. Abdun-Nur, S.G. Barton et al., *Standard Practice for Selecting Proportions for Normal, Heavyweight, and Mass Concrete (ACI 211.1-91)* (American Concrete Institute, Farmington Hills, MI, 1991)
38. Bureau of Indian Standard (BIS), Concrete Mix Proportioning—Guidelines, IS 10262:2019
39. ASTM C39/C39M-21 (Standard Test Method for Compressive Strength of Cylindrical Concrete Specimens), 2021 2021 Annual Book of ASTM Standards, Vol. 04.02, Concrete and Aggregates, American Society for Testing and Materials
40. Bureau of Indian Standard (BIS), Hardened Concrete—Methods of Test, IS 516 (Part 1/Sec 1): 2021
41. Bureau of Indian Standard (BIS), Method of Test for Splitting Tensile Strength of Concrete—Specification, IS 5816-1999 (Reaffirmed 2018)
42. ASTM C496/496M-17 (Standard Test Method for Splitting Tensile Strength of Cylindrical Concrete Specimens), 2021 Annual Book of ASTM Standards, Vol. 04.02, Concrete and Aggregates, American Society for Testing and Materials
43. ASTM 1202-22E01 (Standard Test Method for Electrical Indication of Concrete's Ability to Resist Chloride Ion Penetration), 2021 Annual Book of ASTM Standards, Vol. 04.02, Concrete and Aggregates, American Society for Testing and Materials
44. M. Alexander, Y. Ballim, J.M. Mackechnie, Durability Index Testing Procedure Manual, Research Monograph No. 4, p. 29 (2018)
45. H. Beushausen, R. Torrent, M.G. Alexander, Performance-based approaches for concrete durability: state of the art and future research needs. Cem. Concr. Res. **119**, 11–20 (2019)

46. M.G. Alexander, Durability performance potential and strength of blended Portland limestone cement concrete. Cem. Concr. Compos. **39**, 115–121 (2013)
47. Y. Dhandapani, T. Sakthivel, M. Santhanam, R. Gettu, R.G. Pillai, Mechanical properties and durability performance of concretes with Limestone Calcined Clay Cement (LC3). Cem. Concr. Res. **107**, 136–151 (2018)
48. K.K. Ramagiri, D.R. Chauhan, S. Gupta, A. Kar, D. Adak, A. Mukherjee, High-temperature performance of ambient-cured alkali-activated binder concrete. Innov. Infrastruct. Solut. **6**, 1–11 (2021). https://doi.org/10.1007/s41062-020-00448-y
49. K. Vijay, M. Murmu, Effect of calcium lactate on compressive strength and self-healing of cracks in microbial concrete. Front. Struct. Civ. Eng. **13**, 515–525 (2019). https://doi.org/10.1007/s11709-018-0494-2
50. M.F.S. Zawad, M.A. Rahman, S.N. Priyom, Bio-engineered concrete: a critical review on the next generation of durable concrete. J. Civ. Eng. Forum. **7**, 335 (2021). https://doi.org/10.22146/jcef.65317
51. B. Tayebani, D. Mostofinejad, Self-healing bacterial mortar with improved chloride permeability and electrical resistance. Constr. Build. Mater. **208**, 75–86 (2019). https://doi.org/10.1016/j.conbuildmat.2019.02.172
52. L. Chaurasia, V. Bisht, L.P. Singh, S. Gupta, A novel approach of biomineralization for improving micro and macro-properties of concrete. Constr. Build. Mater. **195**, 340–351 (2019). https://doi.org/10.1016/j.conbuildmat.2018.11.031
53. S. Stocks-Fischer, J.K. Galinat, S.S. Bang, Microbiological precipitation of $CaCO_3$. Soil Biol. Biochem. **31**, 1563–1571 (1999). https://doi.org/10.1016/S0038-0717(99)00082-6
54. N.N.T. Huynh, N.K. Son, An investigation on the use of *Bacillus subtilis* Hu58 in cement mortar. ASEAN Eng. J. **7**, 1–8 (2017). https://doi.org/10.11113/aej.v7.15489
55. Merck KGaA, IR Spectrum Table & Chart, Merck KGaA, Darmstadt, Germany (2022). https://www.sigmaaldrich.com/IN/en/technical-documents/technical-article/analytical-chemistry/photometry-and-reflectometry/ir-spectrum-table. Accessed: 29 June 2022